## **Electron Electric Dipole Moment Searches Using Clock Transitions in Ultracold Molecules**

Mohit Verma<sup>®</sup>, <sup>1</sup> Andrew M. Jayich<sup>®</sup>, <sup>2</sup> and Amar C. Vutha<sup>®</sup>, <sup>1</sup>Department of Physics, University of Toronto, Toronto M5S 1A7, Canada <sup>2</sup>Department of Physics, University of California Santa Barbara, Santa Barbara, California 93106, USA



(Received 3 September 2019; revised 6 March 2020; accepted 10 September 2020; published 8 October 2020)

Permanent electric dipole moments (EDMs) of fundamental particles such as the electron are signatures of parity and time-reversal violation occurring in physics beyond the standard model. EDM measurements probe new physics at energy scales well beyond the reach of present-day colliders. Recent advances in assembling molecules from ultracold atoms have opened up new opportunities for improving the reach of EDM experiments. However, the magnetic field sensitivity of such ultracold molecules means that new measurement techniques are needed before these opportunities can be fully exploited. We present a technique that takes advantage of magnetically insensitive hyperfine clock transitions in polar molecules, offering a way to improve both the precision and accuracy of EDM searches with ultracold assembled molecules.

DOI: 10.1103/PhysRevLett.125.153201

Introduction.—Polar molecules offer one of the best ways to probe the unknown physics that led to the imbalance between matter and antimatter in the Universe [1,2]. Precise measurements using heavy polar molecules, wherein electron spins experience enormous relativistic electric fields, have set stringent bounds on the parity (P) and time-reversal (T) violating permanent electric dipole moment (EDM) of the electron [3-6]—such experiments constrain the parameter space of new physics models out to energy scales exceeding [0,T].

Advances in producing cold molecules [8], such as direct laser-cooling of polar molecules [9-11] and ultracold assembly of molecules from atoms [12-22], have generated interest in applying these techniques to EDM searches [23-27]. Large ensembles of trapped polar molecules can improve experimental sensitivity to P, T-violating physics by more than 2 orders of magnitude, due to the long trap lifetimes (> 10 s) that can be realized. However, it continues to be difficult to directly laser-cool EDM-sensitive molecules—which are typically heavier and have more numerous leakage channels out of the cooling cycle—to the ultracold ( $\lesssim 10 \,\mu\text{K}$ ) temperatures needed to confine them in optical traps [8]. In this context, therefore, an especially attractive and feasible path to producing ultracold trapped molecules is to assemble them from ultracold trapped atoms. A variety of ultracold polar diatomics (mostly bialkali and alkali-alkaline-earth molecules) have been produced in this way ([12–22]), and excellent coherence times for their hyperfine states have been demonstrated [28].

However, an important challenge needs to be overcome before a sensitive EDM experiment with ultracold assembled molecules can be realized. Electron EDM measurements require molecules with unpaired electron spins, which rules out bialkali molecules in their ground states, and thus we are left with molecules with one valence electron such as YbAg (described further below). But the simple  $^2\Sigma$  electronic ground states of these molecules pose problems for traditional EDM measurements: the coherence time of spin precession measurements is degraded by magnetic field noise, and they are susceptible to systematic errors from spurious magnetic fields. Both these disadvantages can be traced back to the relatively large magnetic moment of the unpaired electron spin in these simple diatomic molecules. Therefore it is believed that ultracold assembled molecules are not ideal for EDM searches, and other molecules with more complex level structures must instead be used (cf. [27]).

To address this challenge, we present an EDM measurement technique which can be used with any polar molecule that has magnetically insensitive hyperfine states ("clock states"). Such states are found across a host of polar molecules, including many examples of molecules that can be assembled from ultracold atoms [29]. Importantly, therefore, our technique unlocks the full potential of ultracold assembled molecules for precise EDM measurements with long coherence times, in aid of the search for new physics at the ~100-TeV energy scale.

Method.—We illustrate the features of our technique using the example molecule <sup>174</sup>Yb<sup>107</sup>Ag. This molecule belongs to a class of electron-EDM-sensitive diatomics whose constituent atoms can be laser-cooled and trapped. We anticipate that YbAg can be produced and trapped in significant quantities at ultracold temperatures in an optical trap, after assembly from ultracold Yb and Ag atoms. YbAg molecules can be synthesized at ultracold temperatures using methods similar to those demonstrated for other isoelectronic molecules (YbLi [20], YbRb [12], and YbCs

[19]). We focus on YbAg due to the larger electronegativity of Ag compared to the alkali atoms, which results in a more strongly polar molecule with enhanced sensitivity to the electron EDM [25]. In the  $^2\Sigma$  electronic ground state of YbAg, the lowest rovibrational manifold contains four hyperfine states obtained by coupling the valence electron spin (S=1/2) to the Ag nuclear spin (I=1/2). The interaction Hamiltonian for these states with external electric and magnetic fields is

$$H_I = -\mu_B(g_s \vec{S} + g_I \vec{I}) \cdot \vec{B} - D\hat{n} \cdot \vec{\mathcal{E}} + W_{PT} \vec{S} \cdot \hat{n} \quad (1)$$

(with  $\hbar=1$  everywhere),  $g_S$ ,  $g_I$  are the electron and nuclear spin g factors, D is the molecular dipole moment, and  $\hat{n}$  is the unit vector pointing along the internuclear axis of the molecule. The electron EDM, and other sources of P, T-violation such as the scalar-pseudoscalar nucleon-electron interaction [30], are described by the effective low-energy Hamiltonian  $W_{PT}\hat{S}\cdot\hat{n}$ .

In EDM search experiments, a lab electric field,  $\vec{\mathcal{E}} = \mathcal{E}_z \hat{z}$ , polarizes the molecule and a small magnetic field,  $\vec{\mathcal{B}} = \mathcal{B}_z \hat{z}$ , is used to control the electron spin. A molecule polarized in an electric field has a nonzero expectation value of its orientation,  $\zeta = \langle \hat{n} \cdot \hat{z} \rangle$ , and the effective interaction Hamiltonian for the electron and nuclear spin degrees of freedom can be expressed as

$$H_{\text{eff}} = -(g_s S_z + g_I I_z) \mu_B \mathcal{B}_z + W_{PT} S_z \zeta. \tag{2}$$

The dependence of the molecular orientation  $\zeta$  on the applied electric field  $\mathcal{E}_z$  is discussed in detail in the Supplemental Material [29], using both a detailed numerical model and a simple analytical model. In the traditional EDM measurement method, a static electric field is applied and the energy difference between the  $F=1,\ m_F=\pm 1$  hyperfine levels due to the  $W_{PT}$  term is measured, typically using a spin-interferometer sequence [3,6,31,32]. However, the magnetic field sensitivity of the  $m_F\neq 0$  levels leads to the coherence time limitations and systematic errors mentioned above.

In our proposed clock transition (CT) method, we instead focus on the two hyperfine clock states  $|g\rangle \equiv$  $|F=0, m_F=0\rangle$  and  $|e\rangle \equiv |F=1, m_F=0\rangle$ , which are separated in energy by  $\omega_0$ . Despite the fact that both of these states have zero spin (and thus zero magnetic moment), they can remarkably still be used to measure the EDM associated with the electron spin, as we demonstrate below. We consider the interaction of the molecule with a time-dependent polarizing electric field,  $\mathcal{E}_z = \mathcal{E}_0 \cos(\omega_E t + \beta)$ , and a time-dependent magnetic field,  $\mathcal{B}_z = \mathcal{B}_0 \cos(\omega_B t)$ , where  $\beta$  is an adjustable phase. The magnetic field drives the hyperfine clock transition between  $|q\rangle$  and  $|e\rangle$ . The electric field induces an oscillating molecular orientation with amplitude  $\zeta_0$  at the frequency  $\omega_E$ , as shown in Fig. 1. Because of P, T violation, the molecular orientation behaves like an effective magnetic

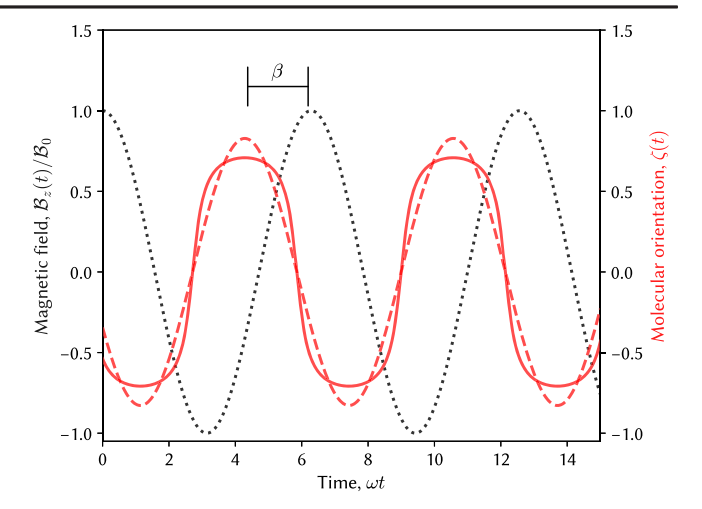


FIG. 1. Magnetic field  $\mathcal{B}_z(t)$  (black, dotted line) and molecular orientation  $\zeta(t)$  (red, solid line). The curve for  $\zeta(t)$  is in response to an electric field  $\mathcal{E}_z(t) = \mathcal{E}_0 \cos(\omega t + \beta)$  and is calculated using the methods in [29], Sec. A. The nonlinear response of  $\zeta$  to  $\mathcal{E}_z$  is evident. The red dashed line shows the first harmonic of  $\omega$  contained in  $\zeta(t)$ , which drives the hyperfine transition.

field coupled to the electron spin [see Eq. (2)]. The key idea is that the P, T-violating term induces an extra transition amplitude between  $|g\rangle$  and  $|e\rangle$ , which interferes constructively or destructively (depending on the phase  $\beta$ ) with the transition amplitude due to the applied magnetic field. The dynamics in the subspace spanned by the clock states is represented on the Bloch sphere in Fig. 2, which illustrates the interference between the transition amplitudes.

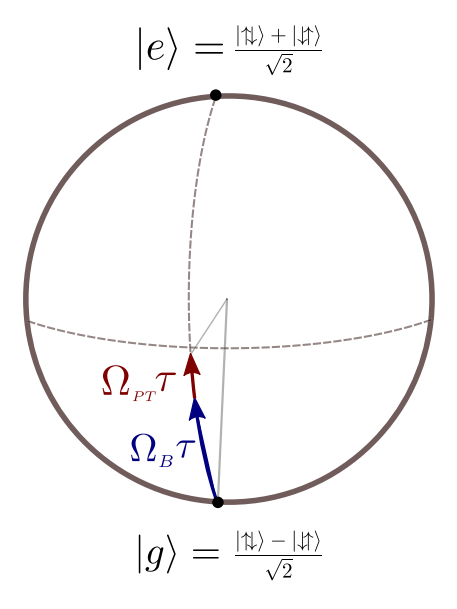


FIG. 2. The population transfer is shown on a Bloch sphere for the two clock states in the presence of oscillating electric and magnetic fields. The P, T-violating Hamiltonian leads to an extra transition amplitude  $\Omega_{PT}\tau$  that interferes with the transition amplitude  $\Omega_B\tau$  due to the oscillating magnetic field. The case shown here corresponds to  $\beta=0$ , where these amplitudes add constructively.

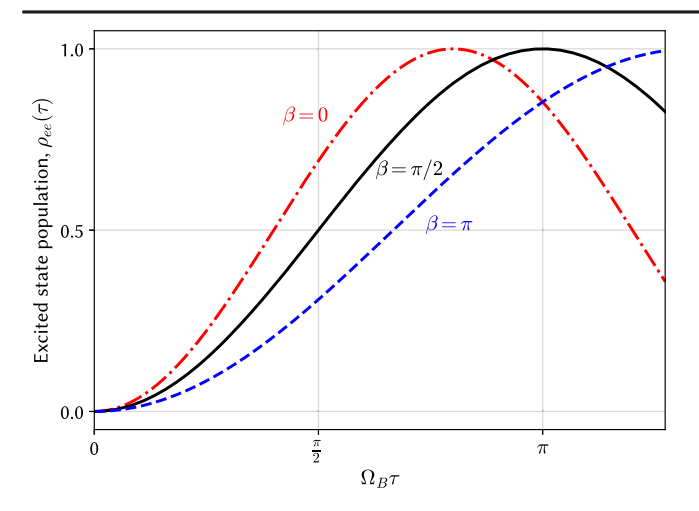


FIG. 3. The population in the excited clock state,  $|e\rangle$ , as a function of interaction time, when the electric and magnetic fields are on resonance ( $\Omega_{PT}$  is exaggerated for illustration). The relative phase  $\beta$  between the electric and magnetic fields can be varied to distinguish the P, T-violating transition amplitude from that due to the magnetic field.

We assume that the electric and magnetic fields are driven at the same frequency,  $\omega_E = \omega_B = \omega$ , with detuning  $\Delta = \omega - \omega_0$ . In the rotating wave approximation, the Hamiltonian from Eq. (2) is

$$H_{\text{eff}} = \frac{\Omega_B}{2} \sigma_x + \frac{\Omega_{PT}}{2} (\cos \beta \sigma_x + \sin \beta \sigma_y) + \frac{\Delta}{2} \sigma_z, \quad (3)$$

where  $\sigma_{x,y,z}$  are Pauli matrices, and the Rabi frequencies for the Zeeman and P, T-violating interactions are  $\Omega_{PT} = \frac{1}{2}W_{PT}\zeta_0$  respectively and  $\Omega_{PT} = \frac{1}{2}W_{PT}\zeta_0$ . When the molecule is driven on resonance ( $\Delta=0$ ) for a time  $\tau$ , molecules initially prepared in  $|g\rangle$  are transferred to  $|e\rangle$ . The excited-state population is then  $\rho_{ee}(\tau) = \sin^2\{[(\Omega_B + \Omega_{PT}\cos\beta)\tau]/2\}$ , where the vanishingly small terms that are quadratic in  $W_{PT}$  have been dropped. The time evolution of  $\rho_{ee}(\tau)$  and the effect of the phase  $\beta$  are shown in Fig. 3.

For an EDM measurement, the magnetic field amplitude,  $\mathcal{B}_0$ , and the pulse duration,  $\tau$ , are set so that  $\Omega_B \tau \approx \pm \pi/2$  mod  $2\pi$ , to make  $\rho_{ee}$  maximally sensitive to  $\Omega_{PT}$ . The measurement is then repeated for different values of the phase angle  $\beta$ , as shown in Fig. 3. Setting  $\beta = \pm \pi/2$  leaves  $\rho_{ee}$  unchanged, and provides a convenient null test. The values of  $\mathcal{B}_0$  and  $\tau$  can also be varied over a large dynamic range while maintaining the condition  $\Omega_B \tau = \pm (\pi/2) \bmod 2\pi$ , which is a useful way to tease out systematic errors. A genuine P, T-violating signal can be identified using the part of  $\rho_{ee}$  that changes sign under switches of (i) the initial state between  $|g\rangle$  and  $|e\rangle$ , (ii) the phase  $\beta$  between 0 and  $\pi$ , and (iii) the pulse area  $\Omega_B \tau$  between  $\pm \pi/2 \mod 2\pi$ .

With measurements on a total of  $N_{\rm tot}$  molecules, and an interaction time  $\tau$  for each measurement cycle, the precision achievable in a projection-noise-limited measurement of  $W_{PT}=2\Omega_{PT}/\zeta_0$  is  $\delta W_{PT}=2/\zeta_0\tau\sqrt{N_{\rm tot}}$ . The corresponding electron EDM precision (assuming that the electron EDM is the only source of P, T violation) is  $\delta d_e=\delta W_{PT}/2e\mathcal{E}_{\rm eff}$ , where  $\mathcal{E}_{\rm eff}$  is the effective electric field experienced by the electron EDM in the molecule [1,2]. For an experiment using the CT method, we estimate an electron EDM sensitivity

$$\begin{split} \delta d_e &= 10^{-31} \ e \, \mathrm{cm} \bigg( \frac{10^4}{N} \bigg)^{1/2} \bigg( \frac{10 \ \mathrm{s}}{\tau} \bigg) \bigg( \frac{10 \ \mathrm{d}}{T} \bigg)^{1/2} \\ &\times \bigg( \frac{20 \ \mathrm{GV/cm}}{\mathcal{E}_{\mathrm{eff}}} \bigg) \bigg( \frac{1}{\zeta_0} \bigg). \end{split} \tag{4}$$

Here N is the number of trapped molecules used per measurement cycle, and T is the total integration time of the experiment. We have used realistic experimental quantities for the nominal values of N,  $\tau$ , and T above, and assumed  $\mathcal{E}_{\rm eff}=20$  GV/cm for YbAg molecules [33]. Applying the above equation to YbRb, a molecule that has been produced by ultracold assembly [12] and has  $\mathcal{E}_{\rm eff}\sim0.7$  GV/cm [34], we estimate that  $\delta d_e\approx3\times10^{-30}~e\,{\rm cm}$  can be reached. An electron EDM measurement with a precision of  $10^{-31}~e\,{\rm cm}$  would improve on the current state of the art by 2 orders of magnitude and probe energy scales well beyond 100 TeV [1,2].

*Advantages.*—Compared to the traditional EDM search method, the CT method has some practical advantages.

First, in the traditional method spurious low-frequency magnetic fields, e.g., from leakage currents, are a common source of systematic errors. However with hyperfine clock transitions, only radio-frequency (rf) magnetic fields, in the spectral range  $\omega_0 \pm 1/\tau$ , can cause shifts of the Rabi frequency. Such magnetic fields are significantly easier to measure, and shield in practice (due to the high effectiveness of eddy current shielding at these frequencies), with consequent improvements to the control of systematic errors.

Second, the phase  $\beta$  between the electric and magnetic fields can be smoothly varied with high precision using standard rf instruments. This eliminates switching transients and discharges, and the resulting magnetic field errors, that are encountered in typical EDM experiments where the sign of dc electric fields has to be switched. A number of potential systematic effects (discussed further below) also have a characteristic dependence on  $\beta$  that is different from the  $\cos \beta$  dependence of the P, T-violating interaction, which thus allows them to be cleanly separated from genuine new physics signals.

Third, the hyperfine levels separated by  $\omega_0$  are insensitive to magnetic field noise and fluctuations to first order. So the requirements for shielding stray magnetic fields and their low-frequency drifts are significantly relaxed

compared to traditional EDM search experiments. This feature can lead to better control over systematics and simplify the design of experiments.

Fourth, the magnetic field insensitivity of the clock states also improves the precision of EDM measurements, since long coherence times for hyperfine state superpositions can be realized [28].

Fifth, the initial state preparation is simple: it is easy to accurately initialize molecules in one of the hyperfine states  $|g\rangle$  or  $|e\rangle$ , compared to preparing the spin-state superpositions used in the traditional EDM measurement method (e.g., [3]). This feature improves the duty cycle of experiments, yielding better precision in a given integration time, and greatly reduces systematic errors due to imperfect state preparation.

Finally, while we have focused on electron EDM measurements for the sake of simplicity, the same method can be used to measure nuclear P, T violation, arising from P, T-violating nuclear moments or new physics interactions between electrons and nucleons [35]. For nuclei in polar molecules, there is in fact an additional term  $H_{nPT} =$  $W_{nPT}I_z\zeta$  in the effective Hamiltonian in Eq. (2), representing the P, T-violating coupling between the nuclear spin I and the molecular orientation. Therefore the CT method can be applied to nuclear P, T violation search experiments in much the same way as above. This method could be especially valuable in experiments that use radioactive nuclei (e.g., <sup>225</sup>Ra [36] or <sup>229</sup>Pa [37]) to take advantage of their enhanced sensitivity, but where only a limited set of molecular species can be efficiently produced from rare isotope sources. The CT method can also be applied to a variety of molecular ions ([29], Sec. E), as ion traps can be engineered so that the secular and micromotion frequencies are well separated from the hyperfine resonance frequency.

Controlling systematic errors.—Stringent control over systematic errors is an important requirement for EDM measurements. Here we consider potential EDM-mimicking effects that are specific to the CT method. One possible source of such errors is the displacement current produced by the oscillating  $\mathcal E$  field, which produces an  $\mathcal E$ -linear magnetic field. These systematic errors can be suppressed by many orders of magnitude, using the characteristic dependence of the P, T-violating signal on the phase  $\beta$  and frequency  $\omega_E$  of the  $\mathcal E$  field ([29], Sec. C).

We have also analyzed other sources of systematic errors, such as E1-M1 mixing and differential Stark shifts. Stray background electric ( $\mathcal{E}_{dc}$ ) and magnetic ( $\mathcal{B}_{dc}$ ) fields can admix rotational states in the N=0 and N=1 manifolds. This leads to a transition Rabi frequency  $\Omega_{E1-M1} \propto \mathcal{E}_{dc}\mathcal{B}_{dc}\mathcal{E}_0$  which can mimic  $\Omega_{PT}$ . For realistic estimates of the stray fields, numerical and analytical calculations described in the Supplemental Material [29] indicate that this effect leads to a negligible systematic error. We have also considered systematic errors that arise through the differential Stark shift of the hyperfine clock states in the oscillating electric field. Using both analytical

and numerical models, we find that the error due to this effect is also negligible ([29], Sec. D).

Finally, we point out that the nonlinear response of the molecular orientation to the  $\mathcal{E}$  field offers up a uniquely powerful way to control any residual systematic errors. This method employs the fact that  $\zeta(t)$  contains odd harmonics of the electric field frequency  $\omega_E$  (see [29], Fig. 5). So  $\omega_E$  can be set to a subharmonic of the hyperfine resonance frequency  $\omega_0$  (e.g.,  $\omega_E = \omega_0/3$ ), while still allowing the P, T-violating interaction to resonantly drive the hyperfine transition. But any systematic effects linear in the electric field (a condition that encompasses the overwhelming majority of them) are pushed far off resonance, and so their interference with the transition amplitude is highly suppressed. Subharmonic modulation therefore offers a clear and general diagnostic to distinguish genuine P, T-violating effects from spurious backgrounds. Precision control of electric and magnetic field amplitudes and phases in the rf domain, in combination with methods such as subharmonic modulation, provides a versatile toolbox to control systematic errors in EDM measurements using hyperfine clock transitions.

Summary.—We have presented a technique for measuring parity and time-reversal violation, which leverages the magnetic-field insensitivity of ubiquitously available hyperfine clock transitions in polar molecules. The use of clock transitions enables longer coherence times leading to improved precision, and opens up new ways to control systematic errors in experiments using trapped ultracold molecules. A wide selection of ultracold molecules, including simple  $^2\Sigma$  diatomic molecules that can be assembled out of ultracold atoms, thus becomes available for new physics searches.

We thank Wes Campbell, Jonathan Weinstein, and David DeMille for helpful comments. M. V. acknowledges support from NSERC and an Ontario Graduate Scholarship. A. M. J. acknowledges support from NSF Grant No. PHY-1912665. A. C. V. acknowledges support from Canada Research Chairs and a Sloan Research Fellowship.

amar.vutha@utoronto.ca

<sup>[1]</sup> D. DeMille, J. M. Doyle, and A. O. Sushkov, Science **357**, 990 (2017).

<sup>[2]</sup> M. S. Safronova, D. Budker, D. DeMille, D. F. J. Kimball, A. Derevianko, and C. W. Clark, Rev. Mod. Phys. 90, 025008 (2018).

<sup>[3]</sup> J. J. Hudson, D. M. Kara, I. Smallman, B. E. Sauer, M. R. Tarbutt, and E. A. Hinds, Nature (London) 473, 493 (2011).

<sup>[4]</sup> J. Baron *et al.* (ACME Collaboration), Science **343**, 269 (2014).

<sup>[5]</sup> W. B. Cairncross, D. N. Gresh, M. Grau, K. C. Cossel, T. S. Roussy, Y. Ni, Y. Zhou, J. Ye, and E. A. Cornell, Phys. Rev. Lett. 119, 153001 (2017).

<sup>[6]</sup> V. Andreev *et al.* (ACME Collaboration), Nature (London) 562, 355 (2018).

- [7] J. L. Feng, Annu. Rev. Nucl. Part. Sci. 63, 351 (2013).
- [8] P. S. Julienne, Nat. Phys. 14, 873 (2018).
- [9] S. Truppe, H. Williams, M. Hambach, L. Caldwell, N. Fitch, E. Hinds, B. Sauer, and M. Tarbutt, Nat. Phys. 13, 1173 (2017).
- [10] A. L. Collopy, S. Ding, Y. Wu, I. A. Finneran, L. Anderegg, B. L. Augenbraun, J. M. Doyle, and J. Ye, Phys. Rev. Lett. 121, 213201 (2018).
- [11] L. W. Cheuk, L. Anderegg, B. L. Augenbraun, Y. Bao, S. Burchesky, W. Ketterle, and J. M. Doyle, Phys. Rev. Lett. 121, 083201 (2018).
- [12] N. Nemitz, F. Baumer, F. Münchow, S. Tassy, and A. Görlitz, Phys. Rev. A 79, 061403(R) (2009).
- [13] P. K. Molony, P. D. Gregory, Z. Ji, B. Lu, M. P. Köppinger, C. R. Le Sueur, C. L. Blackley, J. M. Hutson, and S. L. Cornish, Phys. Rev. Lett. 113, 255301 (2014).
- [14] T. Takekoshi, L. Reichsöllner, A. Schindewolf, J. M. Hutson, C. R. Le Sueur, O. Dulieu, F. Ferlaino, R. Grimm, and H.-C. Nägerl, Phys. Rev. Lett. 113, 205301 (2014).
- [15] J. W. Park, S. A. Will, and M. W. Zwierlein, Phys. Rev. Lett. 114, 205302 (2015).
- [16] M. Guo, B. Zhu, B. Lu, X. Ye, F. Wang, R. Vexiau, N. Bouloufa-Maafa, G. Quéméner, O. Dulieu, and D. Wang, Phys. Rev. Lett. 116, 205303 (2016).
- [17] T. M. Rvachov, H. Son, A. T. Sommer, S. Ebadi, J. J. Park, M. W. Zwierlein, W. Ketterle, and A. O. Jamison, Phys. Rev. Lett. 119, 143001 (2017).
- [18] V. Barbé, A. Ciamei, B. Pasquiou, L. Reichsöllner, F. Schreck, P. S. Żuchowski, and J. M. Hutson, Nat. Phys. 14, 881 (2018).
- [19] A. Guttridge, S. A. Hopkins, M. D. Frye, J. J. McFerran, J. M. Hutson, and S. L. Cornish, Phys. Rev. A 97, 063414 (2018).
- [20] A. Green, J. H. See Toh, R. Roy, M. Li, S. Kotochigova, and S. Gupta, Phys. Rev. A 99, 063416 (2019).
- [21] M.-G. Hu, Y. Liu, D. Grimes, Y.-W. Lin, A. Gheorghe, R. Vexiau, N. Bouloufa-Maafa, O. Dulieu, T. Rosenband, and K.-K. Ni, Science 366, 1111 (2019).

- [22] L. De Marco, G. Valtolina, K. Matsuda, W. G. Tobias, J. P. Covey, and J. Ye, Science 363, 853 (2019).
- [23] A. Sunaga, V. S. Prasannaa, M. Abe, M. Hada, and B. P. Das, Phys. Rev. A 99, 040501(R) (2019).
- [24] J. Lim, J. R. Almond, M. A. Trigatzis, J. A. Devlin, N. J. Fitch, B. E. Sauer, M. R. Tarbutt, and E. A. Hinds, Phys. Rev. Lett. **120**, 123201 (2018).
- [25] T. Fleig and D. DeMille (private communication).
- [26] E. B. Norrgard, E. R. Edwards, D. J. McCarron, M. H. Steinecker, D. DeMille, S. S. Alam, S. K. Peck, N. S. Wadia, and L. R. Hunter, Phys. Rev. A 95, 062506 (2017).
- [27] I. Kozyryev and N. R. Hutzler, Phys. Rev. Lett. 119, 133002 (2017).
- [28] J. W. Park, Z. Z. Yan, H. Loh, S. A. Will, and M. F. Zwierlein, Science 357, 372 (2017).
- [29] See Supplemental Material at http://link.aps.org/supplemental/10.1103/PhysRevLett.125.153201 for discussion of numerical methods, systematic error analysis, and EDM-sensitive molecules with clock transitions.
- [30] E. D. Commins, in *Advances in Atomic, Molecular, and Optical Physics* (Elsevier, New York, 1999), Vol. 40, pp. 1–55, https://dx.doi.org/10.1016/S1049-250X(08)60110-X.
- [31] J. H. Smith, E. M. Purcell, and N. F. Ramsey, Phys. Rev. 108, 120 (1957).
- [32] B. C. Regan, E. D. Commins, C. J. Schmidt, and D. DeMille, Phys. Rev. Lett. 88, 071805 (2002).
- [33] T. Fleig (private communication).
- [34] E. R. Meyer and J. L. Bohn, Phys. Rev. A **80**, 042508 (2009).
- [35] T. E. Chupp, P. Fierlinger, M. J. Ramsey-Musolf, and J. T. Singh, Rev. Mod. Phys. 91, 015001 (2019).
- [36] M. Bishof, R. H. Parker, K. G. Bailey, J. P. Greene, R. J. Holt, M. R. Kalita, W. Korsch, N. D. Lemke, Z.-T. Lu, P. Mueller, T. P. O'Connor, J. T. Singh, and M. R. Dietrich, Phys. Rev. C 94, 025501 (2016).
- [37] J. T. Singh, Hyperfine Interact. **240**, 29 (2019).